ACS APPLIED MATERIALS & INTERFACES

Research Article

www.acsami.org

Catalytic Transformation of Persistent Contaminants Using a New Composite Material Based on Nanosized Zero-Valent Iron

Ishai Dror,*[,†] Osnat Merom Jacov,[†] Andrea Cortis,[‡] and Brian Berkowitz[†]

[†]Department of Environmental Sciences and Energy Research, Weizmann Institute of Science, Rehovot, 76100 Israel

[‡]Earth Sciences Division, 90-1116, Lawrence Berkeley National Laboratory, 1 Cyclotron Road, Berkeley, California 94720, United States

ABSTRACT: A new composite material based on deposition of nanosized zerovalent iron (nZVI) particles and cyanocobalamine (vitamin B_{12}) on a diatomite matrix is presented, for catalytic transformation of organic contaminants in water. Cyanocobalamine is known to be an effective electron mediator, having strong synergistic effects with nZVI for reductive dehalogenation reactions. This composite material also improves the reducing capacity of nZVI by preventing agglomeration of iron nanoparticles, thus increasing their active surface area. The porous structure of the diatomite matrix allows high hydraulic conductivity, which favors channeling of contaminated water to the reactive surface of the composite material resulting in faster rates of remediation. The composite material rapidly degrades or transforms completely a large spectrum of water contaminants, including halogenated solvents like TCE, PCE, and cis-DCE, pesticides like alachlor, atrazine and bromacyl, and common ions like nitrate, within minutes to hours. A field experiment where contaminated groundwater containing a mixture of industrial and agricultural persistent pollutants was conducted together with a set of laboratory experiments using individual contaminant solutions to analyze chemical transformations under controlled conditions.

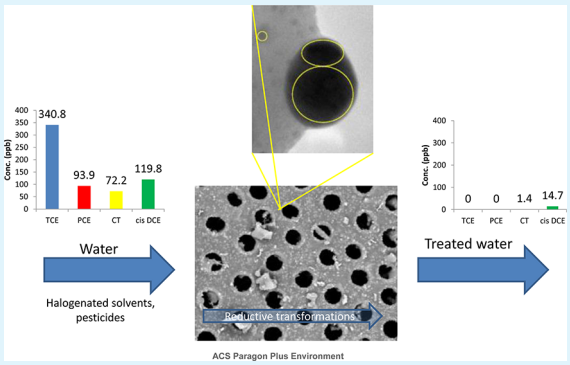

KEYWORDS: *nZVI, chlorinated organics, groundwater contamination, field experiment, diatomite matrix*

INTRODUCTION

Contamination of soil and subsurface regimes is a major problem, with estimates of hundreds of thousands of potentially contaminated sites in both the USA and Europe.[1] These contaminated sites are characterized by many different parameters (from pollutant type and amount to geomorphology and climatic conditions) and therefore multiple technologies are often required to treat them. One of the most promising approaches to simultaneously treat a large variety of contaminants is through reduction, and this approach has been successfully demonstrated for the remediation of contaminated groundwater numerous times.[2−4]

A large set of reducing agents, including mostly elemental metals, has been proposed to enhance or enable the transformation of contaminants. In the last two decades many studies have demonstrated that nanosized zerovalent iron (nZVI) and several other zerovalent metals (e.g., Zn, Al, Mn) act as efficient reducing agents for water contaminants.[5−8] In a review on the use of nanosized iron for environmental remediation, Crane and Scott[8] indicated that nZVI has considerable potential as an effective remediating agent for a large spectrum of contaminants including chlorinated aliphatic and aromatic compounds (e.g., trichloroethylene (TCE), tetrachloroethylene (PCE) and carbon tetrachloride (CT)), pesticides (e.g., DDT and lindane), polychlorinated biphenyls (PCBs), heavy metals (e.g., Cr^{VI}, Pb^{II}, Cd^{II}, and Hg^{II}), and inorganic anions (e.g., dichromate, perchlorate, and arsenate). In most cases, complete reduction of chloro-organic compounds produced environmentally innocuous compounds, whereas reduction of heavy metals rendered them insoluble and immobile.

The degradation or transformation reactivity of zerovalent metals toward various contaminants has been linked to particle size, with larger specific surface areas providing more sites on which reactions can occur.[9−12] However, for nanomaterials enhanced reactivity may also be due to higher density of reactive surface sites and a greater intrinsic reactivity of these surface sites.[7] The advantages of using nZVI include a relatively fast reaction that often completely transforms the contaminants without production of problematic byproduct or intermediates. Furthermore, in a case study of contamination, mainly by PCE and TCE, the cost of remediation using nZVI was estimated to be only about 10 and 20%, respectively, of pump and treat, and permeable reactive barrier (PRB) treatment costs.[13]

In spite of the above-mentioned advantages of nZVI, in many cases nanoparticles agglomerate due to van der Waals and magnetic attraction forces[14] which may lead to the loss of the benefits associated with their innate high specific surface area.[15]

Received: March 6, 2012
Accepted: June 9, 2012
Published: June 10, 2012

   dx.doi.org/10.1021/am300402q | *ACS Appl. Mater. Interfaces* 2012, 4, 3416−3423

Thus, to further improve the reducing capacity of nZVI and to prevent agglomeration of iron, two main approaches have been adopted. The first uses surfactants, or other surface coatings, to increase the repulsive forces between the nanoparticles; this keeps the nanoparticles dispersed in solutions, so that they can be injected into subsurface contaminated zones. This method has been applied at various scales (up to field tests) and its major limitations are that the radius of influence for nZVI injection is only a few meters[16] and that coating of the active material often isolates or interferes with the ability of nZVI to react with contaminants.

The second approach to overcoming agglomeration involves immobilization of nanoparticles on a matrix that can be used either as filling material in a reactive barrier[17,18] or as a carrier that is injected.[19,20] Several different matrix supports have been suggested. Ponder et al.[15] demonstrated enhanced reduction rates of up to 30 times (on a molar basis) for Cr^{VI} and Pb^{II}, by depositing ZVI on a resin. nZVI supported on zirconium oxide and silica gel showed similar results.[21] Meyer et al.[22] demonstrated that incorporating metallic nanoparticles in polymeric cellulose acetate films was capable of stabilizing the growth of 24 nm zerovalent metal nanoparticles. When applied to dechlorination, the hybrid films demonstrated greater TCE reduction rates, using only 10% of the metal loading fraction generally reported in the literature. Immobilization of nZVI on cation exchange resins and subsequent use of the bound nZVI in batch experiments resulted in stepwise debromination of decabromodiphenyl ether (BDE 209).[23] Similar debromination of BDE 209 in a batch system was also demonstrated with nZVI immobilized on mesoporous silica microspheres.[20] Recently, organobentonite was shown to be a good support for nZVI; when suspended in solution, this composite was then demonstrated to degrade pentachlorophenol[24] and atrazine.[25] The use of supports to reduce size of nanoparticle aggregates may also enhance reactivity, by increasing densities of reactive surface sites as well as their intrinsic reactivity.[7]

To date, the application of nZVI at the field scale has been applied only through an injection of a nanoparticle slurry,[3] but not as a reactive barrier or filter where contaminated groundwater is channeled and treated while moving through a matrix containing nZVI. Furthermore, the immobilization of nZVI on highly porous and permeable matrices, to combine the advantages of high reactivity and fast degradation rates of the nZVI − enhanced by the presence of an electron mediator − with favorable hydraulic properties that stimulate flow through the matrix, has not been considered to date for the treatment of contaminated water.

In the current study, diatomite is examined as a potential matrix for nZVI together with cyanocobalamine as an electron mediator and is a naturally occurring, highly structured, fine hydrous silica powder formed from the remains of planktonic algae. Diatomite is also used in many applications because the uniquely porous nature of each nanoparticle gives high surface area, low bulk density, high permeability, high absorption, and low abrasion.[26] It is also chemically inert and almost indestructible except in strongly alkaline conditions. Diatomite is used in a variety of food production applications, in serums and other biotechnology applications, and for filtration and stabilization of pharmaceuticals.

Our objectives in this study were to synthesize a composite material that includes combinations of nZVI and cyanocobalamine supported on a diatomite matrix; to obtain information about the physical, hydraulic and chemical properties of the composite material; and to examine the reductive degradation capacity of the composite material under various conditions up to field scale.

EXPERIMENTAL SECTION

Materials. All chemicals were used as received: $FeCl_3{\cdot}6H_2O$ (98%), cyanocobalamine (vitamin B_{12}) (99%), and diatomite powder from Sigma; sodium borohydride, $NaBH_4$ (98%), and cyclohexane (99.5%) from Aldrich; diphenylcarbazide (97%) and potassium dichromate (99.5%) from Fluka; acetone (99.5%), tetrachloroethylene (PCE) (99%), carbon tetrachloride (CT) (99%), and toluene (99.5%) from Frutarom, Israel; tribromoneopentyl alcohol (TBNPA) (99%) from DSBG, Israel; and argon (99.995%) from Gordon Gas, Israel.

Synthesis of Reducing Complexes Supported on Diatomite Matrix. $FeCl_3{\cdot}6H_2O$ (0.1 mol) dissolved in water (100 mL) and cyanocobalamine solution (9.31 mL of 2 μM) were placed in a 500 mL filter (vacuum) flask in an anaerobic chamber. Diatomite powder (58 g) was then added to produce a slurry that could be mixed by magnetic stirring. Separately, a solution of 0.3 mol $NaBH_4$ in water (100 mL) was placed in a 125 mL amber bottle, in an anaerobic chamber. The two solutions (iron and $NaBH_4$) were transferred to a fume hood and placed on a magnetic stirrer. The reaction was initiated by dropwise addition of $NaBH_4$ solution into the Fe^{3+} solution, while supplying argon gas to the reaction bottle to prevent intrusion of O_2. The reduction of the iron and synthesis of the nanoparticles was completed upon delivering all of the $NaBH_4$ solution, resulting in the precipitation of a black solid (reduced composite powder). After reaction, the solid was transferred to an anaerobic chamber, collected by filtration and washed with 1000 mL water and 200 mL acetone. The solid was dried in the anaerobic chamber using a vacuum pump (<10% (w) H_2O) and stored in closed jars in the anaerobic chamber until used. For comparison, an identical procedure was used to synthesize diatomite with nZVI only; but in this case, no cyanocobalamine was added to the reaction solution.

The above procedure was scaled up to produce 50 kg of the composite material for a pilot experiment. The solutions were added to a stirred reactor and temperature was monitored throughout the reaction and kept below 25 °C by a reactor jacket and water cooling to ensure control of the reaction. During the reaction hydrogen was vented continuously and after the reaction was finished the material was filtered under an argon blanket. The produced material (50 kg) was transferred directly to a large stainless steel column (1.65 m height and 0.4 m inner diameter) and water was added to fill the column before it was sealed and transferred to the field.

In this study, cyanocobalamine was used as an electron mediator. Electron mediators such as metalloporphyrins and their derivatives such as metallochlorins and metallocorrins (i.e., cyanocobalamine) are known for their ability to catalyze redox reactions and facilitate electron transfer. Previously, we have shown that metalloporphyrins improve and enhance the reduction rate of nZVI for the reduction of chlorinated aliphatic compounds.[27]

Batch Experiments. Degradation of various environmental contaminants (PCE, TBNPA) was studied in 40 mL clear glass vials with PTFE caps. In addition to the reaction samples containing diatomite deposited with nZVI, cyanocobalamine and contaminant solution, the vials included a control containing only clean diatomite and contaminant solution (hereafter referred to as the "control"). To reduce losses caused by evaporation of contaminants, each treatment involved preparation of a set of several vials containing 15 mL of solution containing 50 mg/L contaminant and 1.5 g of nZVI deposited on clean diatomite; all vials were sealed at the beginning of the experiment and opened only for analysis (and thus sacrificed). During analysis, comparisons between the control and test were made to eliminate the effect of headspace losses. Vials were prepared in an anaerobic chamber (Coy) and the vials were shaken at a rate of 150 rpm throughout the experiment. At each time interval, two vials from each treatment were opened and the solution was extracted immediately by adding cyclohexane or toluene (3 mL) for PCE and TBNPA, respectively. The extract was collected and then analyzed.

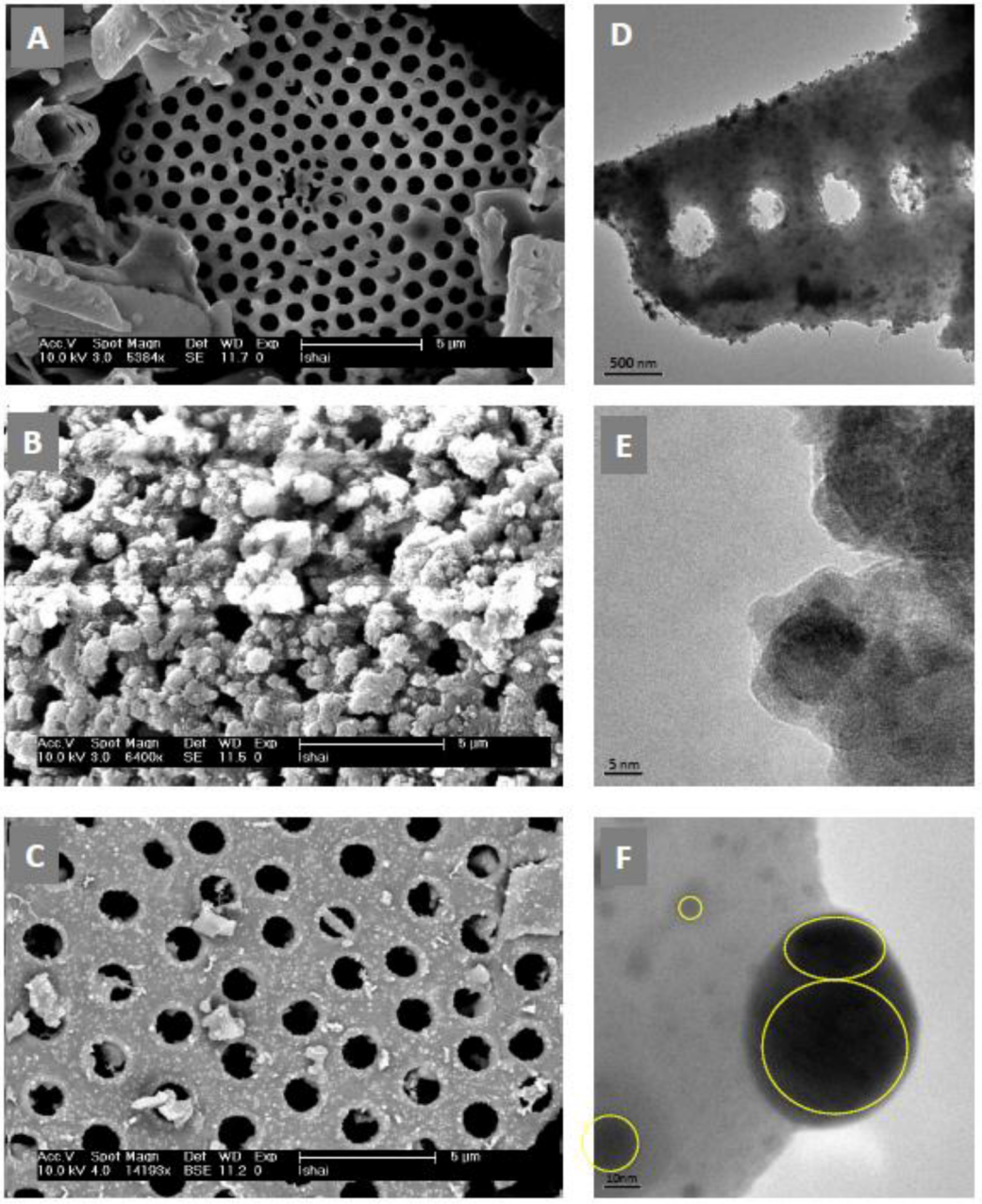

Figure 1. Scanning and transmission electron microscope (SEM, TEM) images: (A) SEM of clean diatomite, (B) SEM of nZVI deposited on diatomite without cyanocobalamine, (C) SEM of nZVI deposited on diatomite in the presence of cyanocobalamine, (D) TEM of nZVI deposited on diatomite in the presence of cyanocobalamine, (E) TEM image showing layer structure of nZVI on the diatomite, and (F) TEM image of several nZVI particles deposited on the diatomite.

Flow Experiments. A sample of contaminated well water from the Nir Galim field site was collected and run in laboratory flow experiments to check field experiment parameters. The cylindrical column had a length of 15 cm and an internal radius of 1.7 cm, and was packed with dry composite material. Three flow rates (Q = 9.4, 6.3, and 4.7 mL/min) were used, corresponding to retention times of 14.5, 21.5, and 29 min, respectively. Samples were collected at the inlet and outlet for each flow experiment and sent for analysis of volatile organic compounds (VOCs) in a certified laboratory (Israel Ministry of Health).

Field Pilot Scale Experiment. The Nir Galim site located in the southern coastal aquifer region of Israel, about 20 km south of Tel Aviv, was selected to test the composite material. The groundwater at the site was contaminated from a nearby industrial zone, primarily from a pesticide manufacturing facility.[28] A combination of several chlorinated compounds and pesticides at high concentrations had previously been identified in the Nir Galim groundwater and soil about 30 years ago.[28] Over many years, the fields around the site were used for agriculture, and many agrochemicals were therefore applied as nonpoint (diffuse) sources which also reached the groundwater. Currently, the groundwater is being pumped and treated by activated carbon reactors at the site. During the experiment a large stainless steel column (1.6 m height and 0.4 m inner diameter) containing composite material (50 kg) was placed near the groundwater treatment facility and 26 m^3 of well water was directed through it over a period of 60 days. During the experiment the flow rate in the column was varied between 63 and 114 L/h to study the effect of residence time. Inlet and outlet samples were collected periodically and sent for analysis.

Chromatographic Analysis. Batch systems were analyzed for PCE and TBNPA concentrations. The extracts from the aqueous batch

experiments were analyzed by Gas Chromatograph coupled to Mass Spectrometer - GC-MS (Varian-Saturn 2000) for qualitative analysis of each reaction product, and by Gas Chromatograph (HP5890) equipped with EC detector and DB 5 ms column (25 m, 0.25 mm, 0.25 μm) for quantitative analysis and kinetic studies. The separation parameters for the studied compounds were: initial temperature of 50 °C for 2 min, ramp of 17 °C/min to 190 °C for 1 min for PCE and 200 °C for 1 min, ramp of 10 °C/min to 250 °C for 4 min for TBNPA. In both cases, the injector and detector temperatures were 220 and 300 °C, respectively.

Samples from the flow experiments were sent for analysis by a certified laboratory (Israel Ministry of Health) using EPA method 524.2[29] for VOCs. Nitrate analysis was performed by IC using method SM 4110 B.[30]

Scanning Electron Microscopy (SEM) Analysis. A JEOL 6400 model equipped with a tungsten filament electron source was used to observe the morphology of the produced materials, and an energy-dispersive spectrometer (EDS; LINK, Oxford) was used for non-destructive elemental analysis and elemental distribution study of microareas.

Transmission Electron Microscopy (TEM) Analysis. A Philips CM120 Super Twin (120 kV, tungsten/LaB6) with EDS for elemental analysis, using a retractable Si(Li) detector with super ultrathin window (EDAX) capability, was used for high resolution measurements to a point resolution of 3.0 Å. Sample preparation for TEM analysis consisted of placing an aliquot of composite material in an aqueous solution, shaking the solution for several minutes and allowing the diatomite to deposit onto a copper grid in a graduated column.

XPS Analysis. A X-ray photoelectron spectrometer (XPS), model Axis-HS (Kratos Analytical) was used to determine surface composition of the material.

Hydraulic Conductivity. A falling head method was used to determine the hydraulic conductivity.[31] The reported values correspond to the mean and standard deviation of ten measurements.

RESULTS AND DISCUSSION

Reactive Matrix Properties. The choice of diatomite as the matrix material was based on the combination of its structural properties (high porosity and hydraulic conductivity) and its stable amorphous silica chemical structure. Immobilization of nZVI particles in the presence of cyanocobalamine, on a porous material with large surface area, results in a composite that can be used for rapid treatment of contaminated water under high flow rates. The diatomite composite with nZVI and cyanocobalamine had hydraulic conductivity of $8.5 \pm 0.6 \times 10^{-6}$ m/s. In comparison, hydraulic conductivity of typical porous material relevant for groundwater ranges from 1×10^{-11} to 1×10^{-8} m/s for clay, to 1×10^{-5} to 1×10^{-3} m/s for well-sorted sand.[31,32] Thus the hydraulic conductivity achieved for the diatomite composite is comparable to that of sand, and may therefore be suitable for use with in situ permeable reactive barriers as well as ex situ reactors.

Representative samples of clean diatomite, diatomite composite with nZVI only, and diatomite composite with ZVI and cyanocobalamine, examined by SEM, are presented in Figure 1A–C. For the materials synthesized after addition of cyanocobalamine (Figure 1C), much smaller nanoparticles are visible, with diameters usually smaller than 50 nm. In comparison, for the material synthesized without the electron mediator (Figure 1B) much larger iron aggregates with diameters $\geq$1 μm are visible and many of the pores are blocked by these aggregates. A similar observation of the effect of the catalysts on the morphology of the matrix was found also in our previous work with a different silica matrix.[27] This result indicates that the electron mediator has an important role on the deposition and growth of nZVI particles, resulting in distribution of many small nanoparticles (having diameter of the order of a few tens of nanometers) on the silica skeleton. One explanation is that the nanoparticles adhere to the diatomite surface by interactions between the negatively charged diatomite surface[33,34] (or sites on the diatomite surface) and the iron in solution. Around these sites the nZVI particles are formed as the $NaBH_4$ is added. Furthermore it is suggested here that when added as a catalyst, the cyanocobalamine, which is active in the degradation of water contaminants, also plays a role in reducing nZVI agglomeration and facilitating distribution of the nanoparticles. During the reduction reaction of the iron and the formation of nZVI particles, the cyanocobalamine appears to act as a surfactant that can either (i) disperse the nanoparticles in solution, leading to a large distribution of small nanoparticles, or (ii) coat the nanoparticles and halt the growing process, preventing agglomeration of iron as shown in Figure 1B. Therefore, it is expected that the active complex material formed by the deposition of nZVI and cyanocobalamine will display the same high hydraulic conductivity as the pure diatomite, while its chemical activity will be very high due to the distribution of the nZVI particles on the surface. It should be further noted that we have previously compared the reductive dechlorination activity of nZVI to the activity of nZVI together with cyanocobalamine.[27] It was shown that the presence of cyanocobalamine substantially increases both the total degradation and the rate of the reactions.

Transmission electron microscopy (TEM) analysis was also performed to examine the nature of the nZVI particles on the composite material. Figure 1D presents these nanoparticles at a relatively low magnification scale of 500 nm; darker, iron-rich regions are visible on a lighter silica background. TEM analysis is limited to samples which allow penetration of the electron beam, i.e., thickness less than 50 nm. Therefore, attention was focused on the material observed on the perimeter of the diatomite pores. The darker spots (iron) are observed on the entire surface of the diatomite, and their average diameter is between 10 and 30 nm.

At higher resolution (Figure 1E), crystalline structures are observed both in the silica background and the iron spots. Typical crystal layer spacings measured on the TEM images (and on their FFT transforms) were 2.9 and 4.9 Å. Usually, the diatomite consists of amorphous silica which lacks crystalline structure; however, here crystalline structures are evident on the diatomite surface after the synthesis and are therefore attributed to the nZVI particles.

Elemental analysis for diatomite with cyanocobalamine and nZVI showed the presence of iron, silicon, oxygen and to a smaller extent, cobalt, aluminum and zinc. (Copper was also found; its source was from the sample holder grid.) Quantitative analysis yielded the distribution of elements shown in Table 1. The first TEM samples (results shown in second column of Table 1) were not kept under anaerobic conditions but rather in water suspension – a ratio of 19.9 Si to 55.6% O and 22.6% Fe was found. Even if we assume that only a small amount of the oxygen is related to residual water molecules and most of the oxygen originates from the SiO_2 surface and from oxidized iron species, the balance of Si and Fe to O confirms that there is a substantial amount of zerovalent iron in the sample. This indicates that the nZVI is oxidized relatively slowly in water suspension, even if no special care is taken to keep the samples anaerobic. It was also observed that

Table 1. EDS Analysis for Samples of Diatomite Composite with Cyanocobalamine and ZVI Taken from Water Suspension and from Dry Anaerobic Preparation Sample

element	% sample from water suspension	% sample from dry anaerobic preparation
O	55.6	44.6
Al	0.3	0.7
Si	19.9	26.7
Fe	22.6	25.9
Co	0.8	1.1
Zn	0.8	1.0
Total	100	100

the ratio of Si atoms to Fe iron on the surface is almost 1:1 in both cases, which indicates a coverage of the surface by the iron nanoparticles that is much larger than the atomic ratio of iron in synthesis (less than 10%). The second TEM sample, with data given in Table 1, was prepared from dry, unsorted material and attached (by contact) to the TEM grid. In this case the composite material was kept under anaerobic conditions until TEM sample preparation, and sample analysis was carried out within 2 h. The ratio of oxygen in the sample decreased to 44.4%, and the Si and Fe percentages increased. It was also found that the iron spots were spherically shaped with a diameter <50 nm. The crystalline structure of the iron spots could not be measured directly, because the resolution of the instrument (2.6 Å) was larger than the layer spacing characteristic of elemental iron. However, an indirect measurement of the layer spacing is possible by electron diffraction analysis. The FFT signal interpretation gave a characteristic layer spacing of about 1.9 Å. The crystalline structure of nZVI was reported by Wang and Zhang,[35] and further discussed by O'Carroll et al.,[36] for the same synthesis as used in our study. Comparison of the two TEM samples seems to indicate that the state of oxidation of the iron influences the surface structure properties and the size, shape and orientation of the crystals. However, in both cases a nanosized crystal structure is observed.

XPS analysis of the diatomite containing nZVI and cyanocobalamine showed that the upper layer of the surface iron was in the oxidized form of Fe_2O_3, in accord with previous findings for nanosized iron particles.[7] This layer is estimated to have a thickness of 5−10 nm, and is thought to coat an elemental iron core. The existence of an oxidized layer is explained by exposure to oxidizing agents, mainly dissolved oxygen, which reacts with the reduced iron on the interface. Support for this finding can be seen in Figure 1F, where a TEM image of one relatively large cluster and several smaller clusters in the background are visible. The edges of the iron cluster (delineated by drawn ellipsoids) have a lighter color, which represents a different electron density that can result from different iron species. The XPS analysis also indicated that the amount of iron on the surface was equal to the amount of silica. This illustrates the large coating capacity of the iron on the diatomite interface. Although the iron content of the matrix is less than 10% by weight, it covers ∼50% of the silica surface of the diatomite. In addition, other contaminants including boron and carbon (which might appear during synthesis of the material and the acetone wash) were found on the diatomite surface.

Laboratory Experiments. A series of batch experiments was performed to assess the degradation rate of some representative halogenated compounds, and to determine kinetics of the degradation process. Each batch reactor contained aqueous solutions of halogenated compound together with diatomite, or composite diatomite material. The first target compound was tetrachloroethylene (PCE); concentrations normalized to the control are given in Figure 2A. In a parallel experiment, the degradation of tribromoneopentyl alcohol (TBNPA), a known brominated contaminant with a half-life of 100 yr and halogenated byproducts,[37] was also demonstrated (Figure 2B). A steep first-order reduction in concentration was observed for both PCE and TBNPA, while the controls remained stable throughout the experiments. The first-order decays were found to have almost the same degradation rate (K_{obs} = 1.62 × 10^{-2} L/min and 2.07 × 10^{-2} L/min, respectively). A similar reaction rate for PCE degradation was reported in the literature for nZVI.[38] The surface area of the nanoparticles cannot be measured directly without the surface area of the matrix, but on the basis of the SEM and XPS analyses, we assume that it is approximately 30 m^2/g. This value is comparable to the surface area of the nZVI,

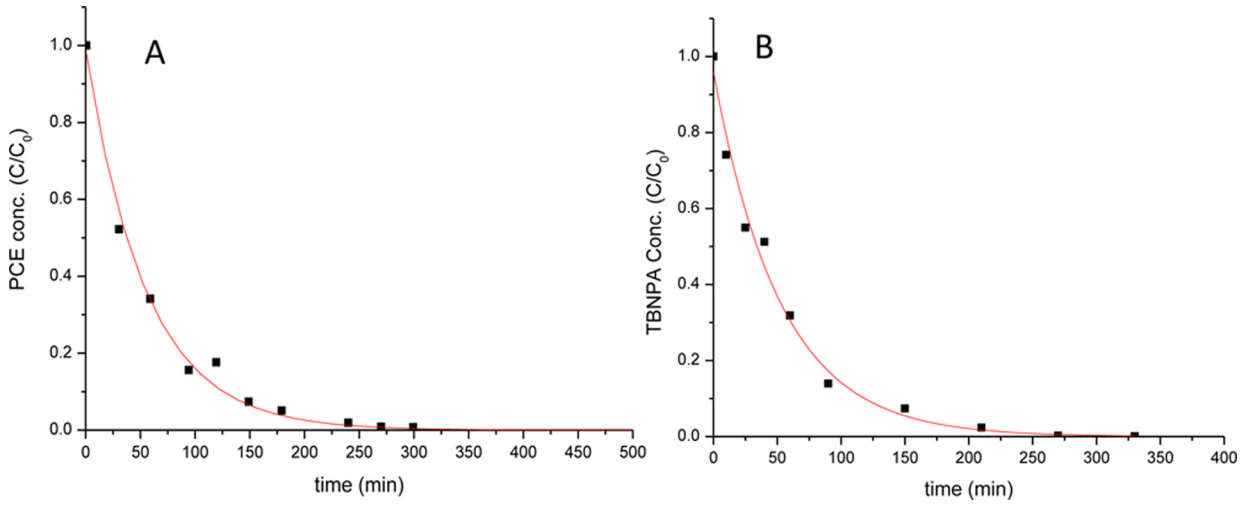

Figure 2. Normalized concentration of (A) tetrachloroethylene (PCE), and (B) tribromoneopentyl alcohol (TBNPA) as a function of reaction time. Solid lines represent a first-order exponential decay fit.

alone, synthesized by the same procedure ($NaBH_4$ reduction). In this latter case, the results fit the published surface area normalized reduction rate for chlorinated aliphatics (e.g., $K_{sa} \approx 4.8 \times 10^{-3}$ L/m^2/min).[7] From the batch results, it is clear that the immobilization of nZVI on the matrix does not decrease its activity, and that use of the composite material in a batch reaction results in degradation of the target compounds.

Subsequently, a sample of contaminated well water from the Nir Galim site was tested in the laboratory in a flow-through column containing the composite material, to examine the ability to treat contaminated water. Figure 3 presents the effect

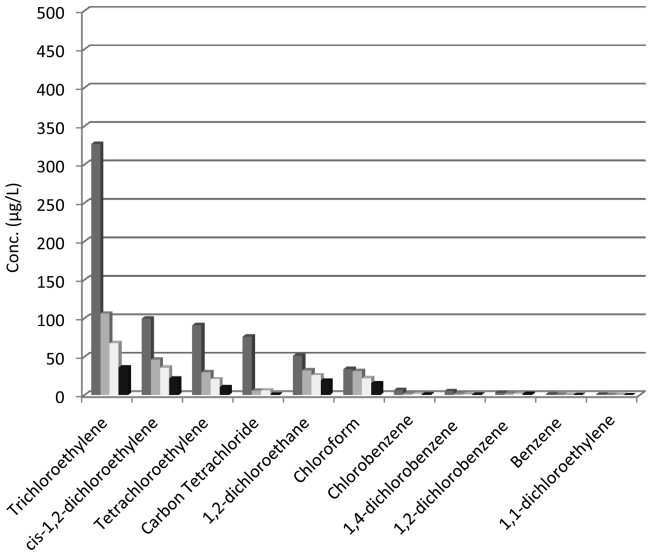

Figure 3. Degradation of Nir Galim groundwater contaminants in column flow-through experiments, as a function of residence time; dark grey, initial groundwater concentrations − water collected from the well; light grey, contaminant concentrations at the column outlet with residence time of 14.5 min; white, contaminant concentrations at the column outlet with residence time of 21.5 min; black, contaminant concentrations at the column outlet with residence time of 29 min.

of residence times on the degradation of several chlorinated organic compounds found in the Nir Galim well water. In all cases, fast and substantial degradation was observed. For example, TCE concentrations decreased from an initial concentration of 327 μg/L to 106, 68, and 36 μg/L for residence times of 14.5, 21.5, and 29 min, respectively. Similarly, carbon tetrachloride concentrations decreased from 76.3 μg/L to 9, 6.2, and 0.9 μg/L for residence times of 14.5, 21.5, and 29 min, respectively. For less chlorinated compounds analyzed in parallel, slower reduction rates were observed. For example, an initial chloroform concentration of 34.2 μg/L decreased to 31.4, 22.1, and 15.5 μg/L for residence times of 14.5, 21.5, and 29 min, respectively. This can be explained by production of chloroform as a byproduct of carbon tetrachloride degradation, and in parallel degradation of chloroform to less and non-chlorinated compounds. This combined process requires a longer reaction time in order to degrade not only the residual concentration but also the byproduct. Overall, the experiment showed that contaminated well water containing a variety of chlorinated compounds can be treated effectively by passing the solution through a column with a residence time of less than 30 min. This residence time was sufficient to substantially degrade many of the chlorinated compounds, notwithstanding the fact that the water also contained many other compounds such as dissolved organic matter, salts, nitrates and pesticides.

Field Experiment. Following the laboratory experiments, a large column was manufactured and charged with 50 kg of the composite material. The column was placed in the Nir Galim field site and flow from the contaminated well water (which is treated and used for industrial purposes) was directed to the column. This field experiment proceeded for 60 days, and samples of the water entering and leaving the column were collected and analyzed for the presence of contaminants. Inlet and outlet concentrations of chlorinated compounds at different times are given in Table 2. High levels of TCE, PCE, cis-DCE, carbon tetrachloride, and chloroform were observed at the inlet. Because such variations were expected at the field scale the results discussed here compare inlet and outlet concentrations or relate total amount degraded during the experiment. The nitrate inlet concentration in the well water averaged 66 mg/L. The residence time in the column throughout the experiment was less than 1 h.

At day 5, most of the chlorinated compounds were degraded; for example, the inlet and outlet TCE concentrations were 340.1 and below detection limits μg/L, respectively. Similarly, PCE inlet concentrations of 93.9 μg/L decreased to below detection limits, while carbon tetrachloride concentrations decreased from 72.2 to 1.40 μg/L. Other less chlorinated compounds, like cis-DCE, chloroform and dichloroethane (which can also be byproduct of PCE, TCE, and carbon tetrachloride degradation) showed major reduction in concentrations. After 17 days from the beginning of the experiment, a

Table 2. Total Degradation Summary over the Experiment in Nir Galim

	day 5 conc. (μg/L)		day 22 conc. (μg/L)		day 46 conc. (μg/L)		
contaminant	inlet	outlet[a]	inlet	outlet	inlet	outlet	total amount degraded (mg)
1,1-dichloroethylene	0.7	<MQL	0.9	0.30	0.7	0.3	10.1
cis-1,2-dichloroethylene	119.8	14.7	104.8	70.90	103.0	91.6	1133.1
chloroform	49.0	18.4	33.0	28.20	28.6	31.5	171.2
1,2-dichloroethane	77.8	36.5	49.7	24.60	45.8	10.8	515.6
carbon tetrachloride	72.2	1.4	90.9	26.70	72.3	35.6	1165.9
trichloroethylene	340.8	<MQL	324.3	139.00	284.3	112.3	4377.0
tetrachloroethylene	93.9	<MQL	105.6	38.60	92.0	32.8	1266.8
chlorobenzene	9.1	2.8	6.0	2.90	5.7	2.1	49.7
1,4-dichlorobenzene	6.4	2.6	4.4	2.20	4.2	1.6	37.0
1,2-dichlorobenzene	1.8	1.3	2.2	1.50	1.4	0.5	4.9

[a]Minimum limit of quantification (MQL) = 0.1 μg/L.

dx.doi.org/10.1021/am300402q | ACS Appl. Mater. Interfaces 2012, 4, 3416−3423

valve in the column was accidentally opened for a short period of time and small amounts of the composite material, gas (mainly H_2) and solution were released from the column, while some oxygen likely entered the column; this led to reduced activity in the column for days 22 and 46. Some activity was still seen up to day 60 when the experiment was terminated.

In both cases, the TCE and PCE concentrations decreased to ~third of their inlet values (324.3 vs 139 μg/L and 105.6 vs 38.6 μg/L at day 22, and 284 vs 112.3 μg/L and 92 vs 32 μg/L, at day 46). The reduction of less chlorinated compounds was also found to occur, but was less effective than prior to opening the valve. The dynamics of PCE, TCE and *cis*-DCE degradation during the experiment are given in Figure 4. The expected

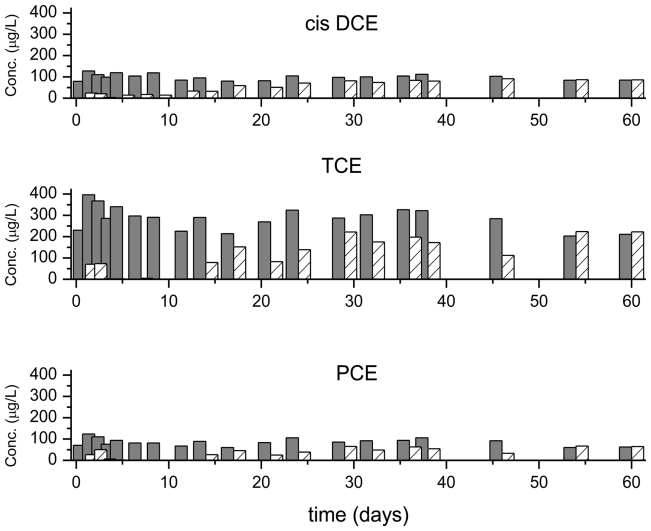

Figure 4. Inlet and outlet concentrations of PCE, TCE, and *cis*-DCE over 60 days of pilot test experiment in Nir Galim well water. grey solid, inlet concentration; striped, outlet concentration.

degradation pathway is PCE → TCE → *cis*-DCE; therefore, it is important to determine if the degradation of PCE and TCE results in complete degradation or, rather, production of chlorinated byproduct. In all cases, it is clear that the degradation of PCE and TCE, which were found in high concentrations, did not produce large amounts of cis-DCE, and that degradation of the highly chlorinated compounds resulted mostly in the production of nonchlorinated compounds. The dynamics of the column activity can be divided into three stages. First, up to day 15, almost all of the chlorinated compounds were degraded. Second, from day 15 to day 54, partial degradation was observed, with higher degradation shown for TCE and PCE relative to *cis*-DCE both in terms of absolute amounts degraded and ratio of inlet to outlet concentrations. In the third stage, days 54–60, almost no degradation was observed. Note that at day 17, which is the start of the second stage, a valve in the column was opened unintentionally for a short period; this also had an impact on the column performance.

The flow rate in the column, which was translated to residence time of solution in the column, had a direct effect on the degradation of the chlorinated compounds (Figure 5). Initially, an increase in degradation rate was observed as the flow in the column was reduced quickly from 114 to 63 L/h. This change led to a sharp increase in the degradation rate from ~65% to over 90%. The following slow increase in flow rate

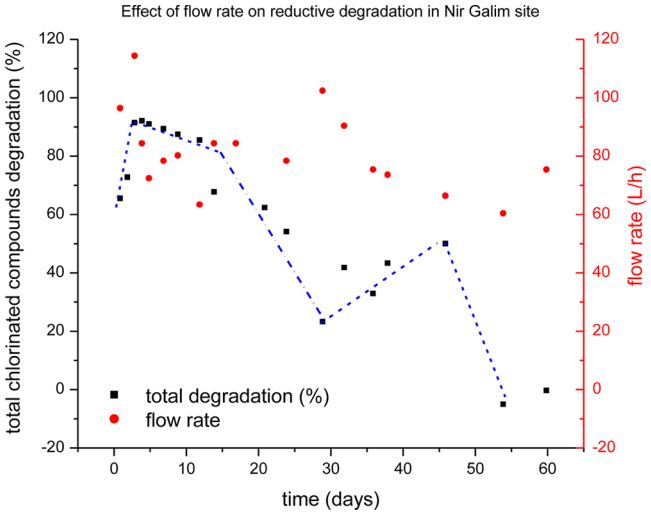

Figure 5. Effect of flow rate on the total degradation of chlorinated compounds (inlet vs outlet).

brought a slow and moderate decrease in degradation rate. Following this period, the valve in the column was opened, which caused perturbations in the flow in the column and a reduction in degradation rate. Even here, a higher flow rate (>100 L/h) showed a low degradation rate (~20%); reducing the flow rate to ~70 L/h caused an increase to more than 50% degradation. At the end—days 54 and 60—in spite of a relatively slow flow rate, the degradation was very low.

Overall, significant chlorinated hydrocarbon degradation was recorded over the 60 days of the experiment, which involved treatment of 26 m^3 of well water. For example, more than 4300 mg of TCE were degraded during the experiment (Table 2).

In addition, the well water was tested for various agrochemicals. The most abundant compound was nitrate, with an inlet concentration of 66.8 mg/L and outlet concentration of 50.1 mg/L. Because the amounts of nitrate were very high (2–3 orders of magnitude larger relative to chlorinated compounds and pesticides), most of the reductive activity of the nZVI was directed to it. In addition to nitrate, pesticides found in the well water were also transformed, as shown in Table 3. For example, bromacyl concentration decreased from 30 to 9 μg/L, and prometryn concentrations decreased to 0.06 μg/L.

CONCLUSIONS

This work has shown that the deposition of nano-ZVI on a matrix in the presence of catalyst prevents aggregation, exposing maximal surface area of the nanoparticles to the treated solution, and that the synthesis of the nZVI composite material can be scaled up from small laboratory production to industrial scale (tens of kg) manufacturing without changing the activity or properties of the resulting material. The resulting material exhibited PCE degradation reaction rates similar to suspended nZVI particles and the hydraulic properties of the composite material enabled flow which resulted in fast treatment of the solution in a flow-through system.

In a field-scale test using contaminated groundwater containing a mixture of contaminants, fast and efficient degradation of contaminants was demonstrated. The material enabled a fast parallel process that degraded halo-organic solvents, pesticides, and nitrates. All measured contaminant concentrations were reduced substantially. TCE, cis-DCE, PCE and DCA carbon tetrachloride and chloroform, which showed

Table 3. Inlet and Outlet Concentrations of Pesticides in Water from the Nir Galim Well

substance	inlet conc. (μg/L)	outlet conc. (μg/L)
simazine	0.7	<0.05
atrazine	0.7	0.3
alachlor	2.6	<0.05
ametryn	3	<0.05
prometryn	7	0.06
bromacyl	30	9
propazine[a]	0.8	0.3
terbutylazine[a]	0.4	0.05
terbutryn[a]	2	ND
dichlorobenzophenone[a]	2	ND
triamterene[a]	25	traces

[a]Values determined based on standards of related compounds.

the largest concentrations in the inlet solution, were degraded to outlet levels that were less than 33%-2% of their inlet concentrations. Many pesticides detected in the contaminated water were also degraded. This study has shown that the synthesis of new composite material based on diatomite matrix and nZVI has potential for the treatment of contaminated water, having demonstrated production and high activity at both the laboratory and pilot scales.

AUTHOR INFORMATION

Corresponding Author

*E-mail: ishai.dror@weizmann.ac.il.

Notes

The authors declare no competing financial interest.

ACKNOWLEDGMENTS

The authors thank Zeev Schwartz for his substantial contribution to the execution of the field experiemnts. B.B. holds the Sam Zuckerberg Professional Chair in Hydrology. The financial support of the European Commission (contract PITN-GA-2008-212298) is gratefully acknowledged.

REFERENCES

(1) Mueller, N. C.; Nowack, B. 2010 Report of the Observatory NANO. Available at www.observatorynano.eu.
(2) Karn, B.; Kuiken, T.; Otto, M. *Environ. Health Perspect.* **2009**, *117*, 1813−1831.
(3) Muller, N. C.; Braun, J.; Bruns, J.; Cernik, M.; Rissing, P.; Rickerby, D.; Nowack, B. *Environ Sci Pollut Res* **2012**, *19*, 550−558.
(4) EPA (2012) Permeable Reactive Barriers, Permeable Treatment Zones, and Application of Zero-Valent Iron: Overview. Available at http://www.clu-in.org/techfocus/default.focus/sec/permeable_reactive_barriers,_permeable_treatment_zones,_and_application_of_zero-valent_iron/cat/overview/ Last updated January 20, 2012.
(5) Gillham, R. W.; O'Hannesin, S. R. *Ground Water* **1994**, *32*, 958−967.
(6) Boronina, T.; Klabunde, K. J.; Sergeev, G. *Environ. Sci. Technol.* **1995**, *29*, 1511−1517.
(7) Nurmi, J. T.; Tratnyek, P. G.; Sarathy, V.; Baer, D. R.; Amonette, J. E.; Pecher, K.; Wang, C.; Linehan, J. C.; Matson, D. W.; Penn, L. R.; Driessen, M. D. *Environ. Sci. Technol.* **2005**, *39*, 1221−1230.
(8) Crane, R. A.; Scott, T. B. *J. Haz. Mat.* **2012**, *211−212*, 112−125.
(9) Yang, G. C. C.; Lee, H. L. *Water Res.* **2005**, *39*, 884−894.
(10) He, F.; Zhao, D. Y. *Environ. Sci. Technol.* **2005**, *39*, 3314−3320.
(11) Kanel, S. R.; Manning, B.; Charlet, L.; Choi, H. *Environ. Sci. Technol.* **2005**, *39*, 1291−1298.
(12) Lien, H. L. K.; Zhang, W. X. *Colloids Surf., A* **2001**, *191*, 97−105.
(13) PARS Environmental. (Dec 2009) An innovative remediation technology for soils and groundwater. http://www.parsenviro.com/nanofeaw-1.html.
(14) Qiu, X.; Fang, Z.; Liang, B.; Gu, F.; Xu, F. *J. Haz. Mater.* **2011**, *193*, 70−81.
(15) Ponder, S. M.; Darab, J. G.; Mallouk, T. E. *Environ. Sci. Technol.* **2000**, *34*, 2564−2569.
(16) Tratnyek, P. G.; Johnson, R. L. *Nano Today* **2006**, *1*, 44−48.
(17) Kim, H.; Hong, H. J.; Lee, Y. J.; Shin, H. J.; Yang, J. W. *Desalination* **2008**, *223*, 212−220.
(18) Li, Z.; Jones, H. K.; Zhang, P.; Bowman, R. S. *Chemosphere* **2007**, *68*, 1861−1866.
(19) Xiong, Z.; Zhao, D.; Pan, G. *J. Nanopart. Res.* **2009**, *11*, 807−819.
(20) Qiu, X.; Fang, Z.; Liang, B.; Gu, F.; Xu, F. *J. Haz. Mater.* **2011**, *193*, 70−81.
(21) Ponder, S. M.; Darab, J. G.; Bucher, J.; Caulder, D.; Craig, I.; Davis, L.; Edelstein, N.; Lukens, W.; Nitsche, H.; Rao, L.; Shuh, D. K.; Mallouk, T. E. *Chem. Mater.* **2001**, *13*, 479−486.
(22) Meyer, D. E.; Wood, K.; Bachas, L. G.; Bhattacharyya, D. *Environ. Prog.* **2004**, *23*, 232−242.
(23) Li, A.; Tai, C.; Zhao, Z.; Wang, Y.; Zhang, Q.; Jiang, G.; Hu., J. *Environ. Sci. Technol.* **2007**, *41*, 6841−6846.
(24) Li, Y.; Zhang, Y.; Li, J.; Zheng, X. *Environ. Pollut.* **2011**, *159*, 3744−3749.
(25) Zhang, Y.; Li, Y.; Zheng, X. *Sci. Total Environ.* **2011**, *409*, 625−630.
(26) Engh, K. R.; *Kirk-Othmer Encyclopedia of Chemical Technology*; John Wiley & Sons: New York, 2000; DOI: 10.1002/0471238961.0409012005140708.a01Article.
(27) Dror, I.; Baram, D.; Berkowitz, B. *Environ. Sci. Technol.* **2005**, *39*, 1283−1290.
(28) Muskat, L.; Lahav, D.; Ronen, D.; Magaritz, M. *Arch. Insect Biochem. Phys.* **1993**, *22*, 487−499.
(29) Munch, J. W. *Methode S24.2 Revision 4.1*; U.S. Environmental Protection Agency: Cincinnati, OH, 1995.
(30) Greenberg, A. E.; Clescerl L. S.; Eaton, A. D. *Standard Methods for the Examination of Water and Wastewater*: 18th ed. supplement; APHA-AWWA-WEF: Washington, D.C., 1994.
(31) de Marsily, G. *Quantitative Hydrogeology*; Academic Press: New York, 1986.
(32) Fetter, C. W. *Applied Hydrogeology*, 2nd ed.; Merrill Publishing:, Columbus, OH, 1988.
(33) Elden, H.; Morsy, G.; Bakr, M. *Asian J. Mater. Sci.* **2010**, *2*, 121−136.
(34) Yuan, P.; Wu, D. Q.; He, H. P.; Lin, Z. Y. *Appl. Surf. Sci.* **2004**, *227*, 30−39.
(35) Wang, C. B.; Zhang, W. X.. *Environ. Sci. Technol.* **1997**, *31*, 2154−2156.
(36) O'Carroll, D.; Sleepc, B.; Krola, M.; Boparaia, H.; Kocura C. *Adv. Water Resour.***2012** doi:10.1016/j.advwatres.2012.02.005
(37) Ezra, S.; Feinstein, S.; Bilkis, I.; Adar, E.; Ganor, J. *Environ. Sci. Technol.* **2005**, *39*, 505−512.
(38) Taghavy, A.; Costanza, J.; Pennell, K. D.; Abriola, L. M. *J. Contam. Hydrol.* **2010**, *25*, 128−42.